Room Temperature Ionic Liquid Based Polystyrene Nanofibers with Superhydrophobicity and Conductivity Produced by Electrospinning

5 AUTHORS, INCLUDING:

XB Lu
Dalian Institute of Chemical Physics
37 PUBLICATIONS **1,532** CITATIONS

SEE PROFILE

Jianhua Zhou
Sun Yat-Sen University
41 PUBLICATIONS **823** CITATIONS

SEE PROFILE

Yihua Zhao
The Hong Kong University of Science and T…
20 PUBLICATIONS **326** CITATIONS

SEE PROFILE

Room Temperature Ionic Liquid Based Polystyrene Nanofibers with Superhydrophobicity and Conductivity Produced by Electrospinning

Xianbo Lu,[†,‡] Jianhua Zhou,[†] Yihua Zhao,[†] Yong Qiu,[†] and Jinghong Li*,[†]

Department of Chemistry, Key Lab of Bioorganic Phosphorus Chemistry & Chemical Biology, Tsinghua University, Beijing 100084, P.R. China, and Dalian Institute of Chemical Physics, Chinese Academy of Sciences, Dalian 116023, P.R. China

Received January 6, 2008. Revised Manuscript Received March 1, 2008

In this report, a polystyrene−ionic liquid (PS-IL) composite nanofiber was successfully produced for the first time by an electrospinning method. The electrospun composite films were characterized by SEM, FTIR, cyclic voltammetry, water contact angle (WCA) measurement, and conductivity measurement. The dimension, morphology, conductivity, and hydrophobicity of electrospun PS-IL composite film can be effectively controlled by altering the experimental parameters for electrospinning, especially the content of IL in the original electrospinning solution. The electrospun PS-IL composite film displayed both superhydrophobicity and conductivity, which may be ascribed to the micro- and nanoscale hierarchical structures of the PS-IL composite film and the intrinsic hydrophobicity and conductivity of the IL (BMIPF$_6$). Entrapment of IL within polymer by electrospinning provides a facile way to create IL-based nanofibers and composite film and may find wide potential applications in the fabrication of controllable and functional surface.

Introduction

Electrospinning is a simple and versatile method for producing micro- and nanoscaled fibers with extremely long length. The electrospun films consisting of a continuous, nonwoven web of nanofibers usually have high surface area and complex pore structure.[1,2] The simplicity of the electrospinning scheme and the diversity of materials suitable for electrospinning, as well as the unique and controllable feature of electrospun fibers and films, all make this technique attractive in the applications of nanofiber-reinforced composite material, nanofiber-based membranes and smart cloth, nanofiber-based sensors and electrode materials, filtration, catalysis, and so forth.[1] Superhydrophobic surfaces (water contact angle, WCA > 150°), which are governed by both the chemical composition and the geometrical microstructure of the surface, are highly attractive for novel industrial and practical applications: continuously clean buildings, stain-resistant fabrics, antifouling marine structures, and oxidation-resistant surfaces.[3] Currently, the production of superhydrophobic surfaces is based on time-consuming, expensive, and/or nonversatile processes, such as controlled crystallization, lithography, etching, and templating.[4] A superhydrophobic surface of electrospun films can be conveniently produced by altering the chemical composition of electrospinning solution and the experimental parameters for electrospinning. However, such a superhydrophobic surface can easily bring about static-charge accumulation, possibly causing a fire or an explosion in practical applications under dry conditions.[3] Fabrication of superhydrophobic surface with good conductivity may be an effective method for eliminating these potential dangers by dissipating the static charge.

Room temperature ionic liquids (RTILs) are compounds consisting entirely of ions that exist in the liquid state around room temperature.[5–7] As a typical RTIL, 1-butyl-3-methylimidazolium hexafluorophosphate (BMIPF$_6$) is a hydrophobic, air-stable, and conductive ionic liquid, which possesses unique properties such as negligible vapor pressure, wide potential windows, high thermal stability, and good conductivity.[7] RTIL-based polymer has attracted much attention in recent years because of its wide potential applications in polymer electrolyte, biosensor, and so forth.[5,6,8,9] Entrapment of IL within polymer by electrospinning provides a facile way to create an IL-based polymer, which might open up new opportunities for the application of IL-based composite materials. An interesting work was reported by Viswanathan et al., in which RTILs were used as nonvolatile solvents to prepare cellulose and cellulose−

* Corresponding author. Tel.: +86 10 6279 5290. Fax: +86 10 6279 5290. E-mail: jhli@mail.tsinghua.edu.cn.
  † Tsinghua University.
  ‡ Chinese Academy of Sciences.

(1) Li, D.; Xia, Y. N. *Adv. Mater.* **2004,** *16,* 1151.
(2) Subbiah, T.; Bhat, G. S.; Tock, R. W.; Parameswaran, S.; Ramkumar, S. S. *J. Appl. Polym. Sci.* **2005,** *96,* 557.
(3) Zhu, Y.; Zhang, J. C.; Zheng, Y. M.; Huang, Z. B.; Feng, L.; Jiang, L. *Adv. Funct. Mater.* **2006,** *16,* 568.
(4) Acatay, K.; Simsek, E.; Yang, C. O.; Menceloglu, Y. Z. *Angew. Chem., Int. Ed.* **2004,** *43,* 5210.

(5) Lu, X. B.; Hu, J. Q.; Yao, X.; Wang, Z. P.; Li, J. H. *Biomacromolecules* **2006,** *7,* 975.
(6) Lu, X. B.; Zhang, Q.; Zhang, L.; Li, J. H. *Electrochem. Commun.* **2006,** *8,* 874.
(7) Buzzeo, M. C.; Hardacre, C.; Compton, R. G. *Anal. Chem.* **2004,** *76,* 4583.
(8) Jiang, J.; Gao, D. S.; Li, Z. H.; Su, G. Y. *React. Funct. Polym.* **2006,** *66,* 1141.
(9) Li, Z. Y.; Liu, H. T.; Liu, Y.; He, P.; Li, J.; Zheng, L. Z.; Li, J. H. *Polymer* **2005,** *46,* 7578.

heparin composite fibers by electrospinning.[10] However, up to now, no work has explored the application of IL in electrospinning for producing IL-based composite material. Polystyrene (PS) is a hydrophobic, air-stable, dielectric, and electrospinable polymer, which has been used to prepare superhydrophobic surfaces by electrospinning.[11–13] Considering the intrinsic hydrophobicity of PS and $BMIPF_6$ and the good conductivity of $BMIPF_6$, the combination of PS and $BMIPF_6$ may be an alternative composite material for the preparation of superhydrophobic film with conductivity. This is the first example of IL successfully entrapped in polymer by electrospinning for producing PS-IL composite nanofibers and film. The electrospun PS-IL composite film displayed both superhydrophobicity and conductivity compared to that of PS and may find potential applications in the fabrication of controllable and functional surface, such as antistatic self-cleaning coating.

Experimental Section

Preparation of Electrospun PS and PS-IL Composite Nanofibers. PS (MW 280 000, from Aldrich) and $BMIPF_6$ (>98%, from Solvent Innovation) were used. The conductivity of pure $BMIPF_6$ was about 1.4×10^{-3} S cm^{-1} at 25 °C.[14] The solution used for electrospinning was prepared as follows: 0.80 g of PS was added to 8 mL of dimethylformamide (DMF) to obtain a homogeneous PS solution with the aid of stirring and sonication, and different volumes of $BMIMPF_6$ (the volume ratio of $BMIPF_6$ to DMF was ranging from 0.1% to 1.5%) were added to the above solution to obtain a PS-$BMIPF_6$ solution. Then the solution (PS or PS-$BMIPF_6$) was immediately loaded into a syringe with a stainless-steel needle (the inlet diameter was about 0.5 mm). A voltage of 16 kV was applied to the needle, and a slide of ITO or aluminum foil was grounded to act as a collecting screen. The distance between the needle tip and collector was 10 cm, and the flow rate of the solution was fixed at 0.1 mL/h. The electrospun nanofibers were collected onto the ITO or aluminum foil to form a thin film, which was used for further characterization.

Charaterization of Electrospun PS and PS-IL Composite Film. The morphological features of the eletrospun films were characterized by a LEO-1530 (Shimadzu, Japan) field-emission scanning electron microscope (FE-SEM). FTIR spectra were obtained on a Perkin-Elmer Spectrum GX spectrometer (Perkin-Elmer Company, U.S.A.). Electrochemical measurements were performed at ambient temperature using a CHI 802 workstation (CH Instruments, Inc., Austin, U.S.A.). The measurements were based on a three-electrode system with the electrospun PS@ITO or PS-$BMIPF_6$@ITO (10-min electrospinning periods) as the working electrode, a platinum wire as the auxiliary electrode, and a saturated Ag/AgCl electrode as the reference electrode. The supporting electrolyte was an aqueous solution containing 1 mM $K_3Fe(CN)_6$ + 0.5 M KNO_3 (in which $K_3Fe(CN)_6$ was a redox probe), and the geometric area of working electrodes was 1 cm^2. The PS@ITO or PS-$BMIPF_6$@ITO working electrode was immersed in the supporting electrolyte for at least 20 min before measurement to ensure complete contact with the supporting

electrolyte. The conductivity of the electrospun PS-$BMIPF_6$ sheet was measured by a sandwich structure using a Keithly 2400 source meter. A thin layer of metal Ag was sputtered onto the surface of the electrospun PS-$BMIPF_6$ sheet to form a square with 0.25 cm^2 geometric surface area, and the electrospun PS-$BMIPF_6$ sheet was sandwiched between the conducting ITO and the metal Ag thin layer. WCAs were measured on a dataphysics OCA20 contact-angle system (Germany) at ambient temperature. Average contact angles were obtained by measuring the same sample at four different positions.

Results and Discussion

Morphological and Spectroscopic Charaterization. Figure 1 shows the SEM images of PS nanofibers and PS-$BMIPF_6$ composite nanofibers with different $BMIPF_6$ content. As can be seen from Figure 1a, the PS nanofibers were very uniform with an average diameter of about 125 nm. The morphology of electrospun PS-$BMIPF_6$ composite nanofibers produced from PS-$BMIPF_6$ solution with 0.1% $BMIPF_6$ content (Figure 1b) was similar to that of PS nanofibers, which did not contain any beads. When the $BMIPF_6$ content in the original solution was increased to 0.5%, the electrospun PS-$BMIPF_6$ composite nanofibers (Figure 1c) became inconsistent with the diameters ranging from tens of nanometers to several hundred nanometers. Previously research revealed that inorganic ionic salts in the original solution could influence the morphology of electrospun fiber.[2,15,16] The charged ions in the polymer solution are highly influential in jet formation in the electrospinning process. The ions increase the charge carrying capacity of the jet, thereby subjecting it to higher tension with the applied electric field. $BMIPF_6$, which consists of organic cations and inorganic anions, is a viscous ionic liquid which has better compatibility and solubility in organic polymer solution than inorganic salts. Usage of IL instead of inorganic salts for the morphological control of eletrospun nanofibers and films may be more desirable. With the increase of $BMIPF_6$ content, the uniformity of PS-$BMIPF_6$ composite fibers became worse and worse and the average diameters of PS-$BMIPF_6$ composite fibers became larger and larger, which was mainly caused by the increasing electric charge introduced by $BMIPF_6$ in the electrospinning solution. When the $BMIPF_6$ content was further increased to 1.5%, the electrospun fibers became severely emanative and were difficult to collect onto the collecting screen. Based on our experiments (the concentration of PS was fixed at about 10%), a good nonwoven electrospun film could be obtained when the volume fraction (V_{IL}/V_{DMF}) of $BMIPF_6$ was not more than 0.75%. It can be concluded from Figure 1 that the dimension and morphology of electrospun PS-IL composite fibers and film could be effectively controlled by altering the content of IL in the original electrospinning solution.

Figure 2 shows the FTIR spectra of electrospun PS nanofibers, PS-$BMIPF_6$ nanofibers, and pure $BMIPF_6$. As can be seen from Figure 2, almost all the characteristic peaks of PS can be found in the PS-$BMIPF_6$ composite nanofibers.

(10) Viswanathan, G.; Murugesan, S.; Pushparaj, V.; Nalamasu, O.; Ajayan, P. M.; Linhardt, R. J. *Biomacromolecules* **2006**, *7*, 415.

(11) Kim, K.; Kang, M.; Chin, I. J.; Jin, H. J. *Macromol. Res.* **2005**, *13*, 533.

(12) Kang, M.; Jung, R.; Kim, H. S.; Jin, H. J. *Colloids Surf., A* **2008**, *313−314*, 411.

(13) Zheng, J.; He, A.; Li, J.; Xu, J.; Han, C. *Polymer* **2006**, *47*, 7095.

(14) Liu, J. F.; Jonsson, J. A.; Jiang, G. B. *TrAC, Trends Anal. Chem.* **2005**, *24*, 20.

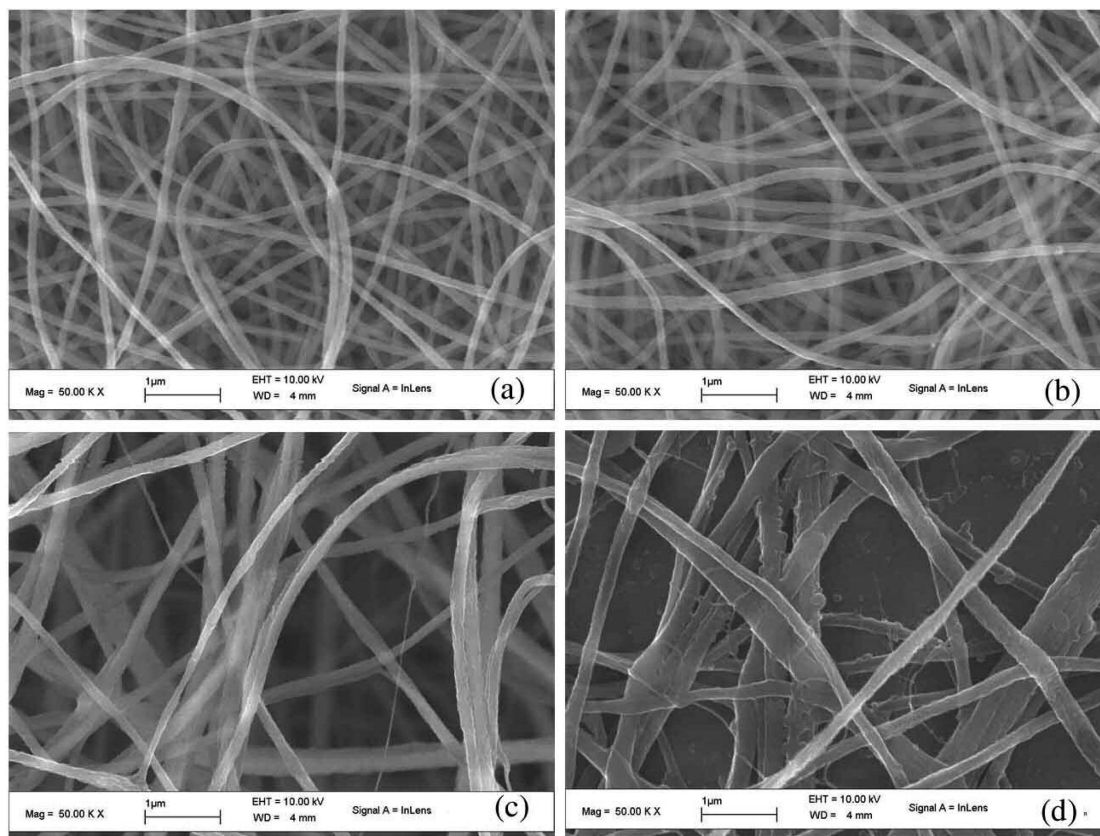(15) Zong, X. H.; Kim, K.; Fang, D. F.; Ran, S. F.; Hsiao, B. S.; Chu, B. *Polymer* **2002**, *43*, 4403.

Figure 1. SEM images of electrospun PS nanofibers (a) and PS-BMIPF$_6$ composite nanofibers with different BMIPF$_6$ content (the volume ratio of BMIPF$_6$ to DMF in the original solution for electrospinning): (b) 0.1%; (c) 0.5%; and (d) 1.5%.
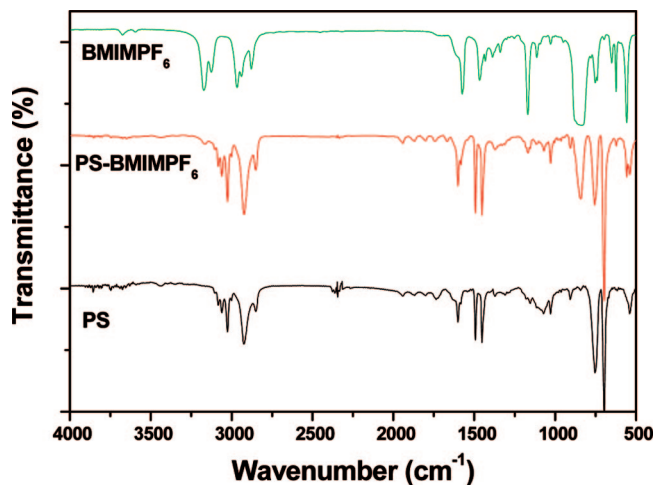

Figure 2. FTIR spectra of electrospun PS nanofibers, PS-BMIMPF$_6$ nanofibers, and pure BMIMPF$_6$.
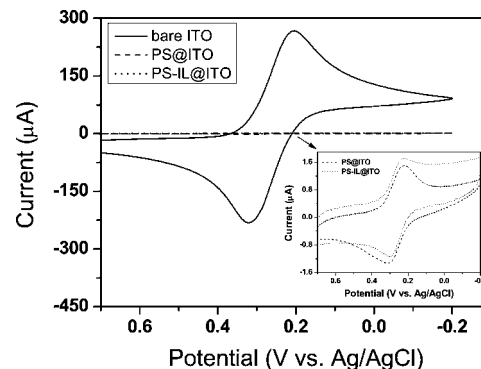

Figure 3. Cyclic voltammograms of PS@ITO, PS-IL@ITO (0.5% BMIPF$_6$ content), and bare ITO with a scan rate of 0.1 V s^{-1}. Inset is the magnified cyclic voltammograms of PS@ITO and PS-IL@ITO. The supporting electrolyte was 1 mM K$_3$Fe(CN)$_6$ + 0.5 M KNO$_3$ aqueous solution (in which K$_3$Fe(CN)$_6$ was the redox probe), and the geometric area of working electrodes was 1 cm^2.

The band at 697 cm^{-1} is assigned to the out of phase ring deformation for monosubstituted aromatic rings. The aromatic C═C stretching vibration peaks appear at near 1602 cm^{-1}. The peaks at 3083, 3061, and 3026 cm^{-1} are all assigned to the aromatic C−H stretching vibration. The peaks assigned to C−H bending vibration appear at 1452 and 1493 cm^{-1}. Meanwhile, the relatively intensive characteristic peaks of BMIPF$_6$ at 835, 624, 1170, and 3172 cm^{-1} can also be found in PS-BMIMPF$_6$ composite nanofibers, which confirmed the presence of BMIPF$_6$ in PS-BMIMPF$_6$ composite nanofibers. The wide intensive absorption peak appearing at near 835 cm^{-1} is assigned to the combinative vibration

of PF$_6^-$ and the P−F bond.[8,17] The frequencies of 3172, 1170, and 624 cm^{-1} are all assigned to the vibration of C−H for cyclic BMI$^+$.[8,17] The characteristic peaks of BMIPF$_6$ were relatively weaker compared to that of PS because the mass ratio of PS to BMIPF$_6$ was about 20:1. By electrospinning, BMIPF$_6$ could be effectively entrapped in the electrospun polymer nanofibers and film.

(16) Kim, S. J.; Lee, C. K.; Kim, S. I. *J. Appl. Polym. Sci.* **2005**, *96*, 1388.
(17) Anbu, N. N.; Sasaki, Y.; Kitamura, F. *Electrochem. Commun.* **2003**, *107*, 7827.
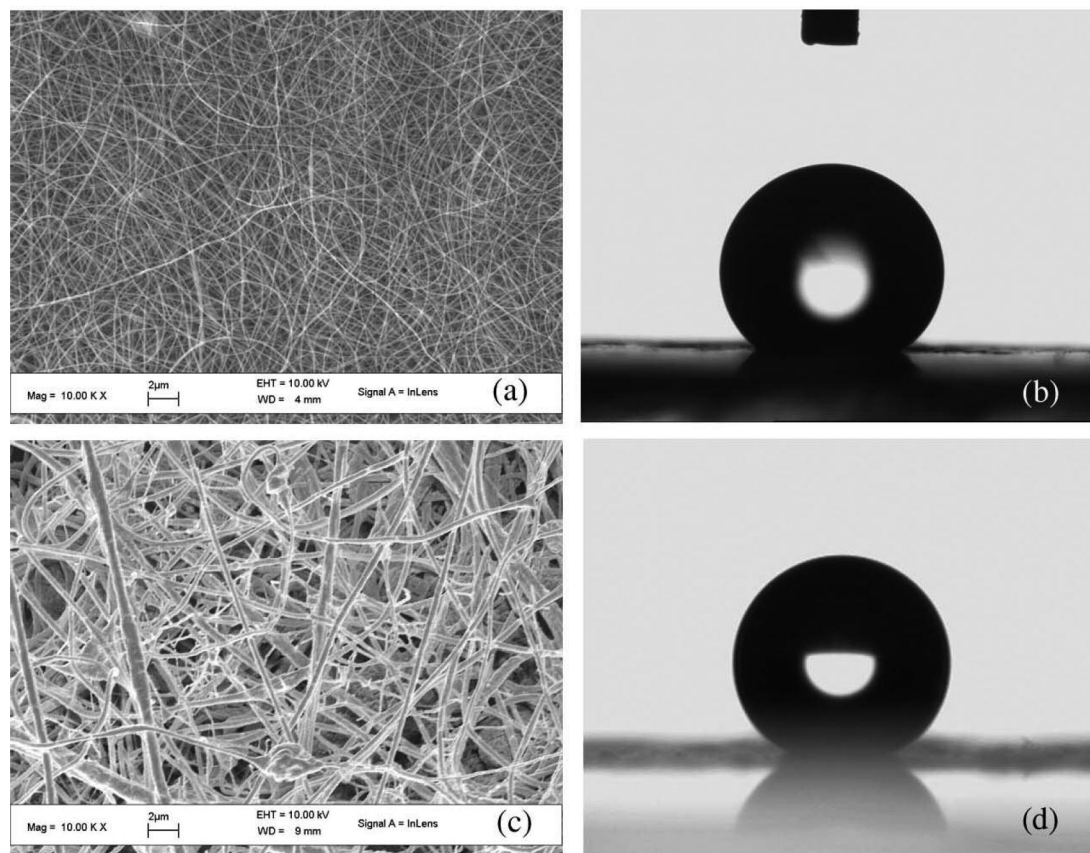(18) Erbil, H. Y.; Demirel, A. L.; Avcy, Y.; Mert, O. *Science* **2003**, *299*, 1377.

Figure 4. SEM images of electrospun PS film (a) and PS-BMIPF$_6$ composite film (c) and the corresponding photographs taken during WCA measurements: (b) electrospun PS film with WCA of 141° and (d) electrospun PS-BMIPF$_6$ composite film with WCA of 153°.

Coverage Degree Investigation of Electrospun Films by Cyclic Voltammetry. The coverage degree of electrospun films on the conducting collecting screen was investigated by the cyclic voltammetric method. The electrospun films of PS and PS-IL (i.e., PS-BMIPF$_6$) were collected onto ITO to obtain PS@ITO and PS-IL@ITO, which were used as the working electrode to estimate the coverage degree of electrospun films. Figure 3 gives the cyclic voltammograms of PS@ITO, PS-IL@ITO, and bare ITO in 1 mM K$_3$Fe-(CN)$_6$+ 0.5 M KNO$_3$ aqueous solution (in which K$_3$Fe(CN)$_6$ was the redox probe). The bare ITO gave a pair of quasi-reversible redox peaks with a cathodic (or anodic) peak current of about 270 μA. Compared with bare ITO, the cathodic peak currents at PS@ITO and PS-IL@ITO were very small. The inset of Figure 3 also gives the magnified cyclic voltammograms of PS@ITO and PS-IL@ITO with a nearly equivalent cathodic peak current of about 1 μA. The electrode coverage (T_c) of electrospun PS@ITO (or PS-IL@ITO) can be calculated as follows:

$$T_c = \frac{i_m - i}{i_m} \times 100\% \qquad (1)$$

where i_m and i are the cathodic (or anodic) peak currents of bare ITO and PS@ITO (or PS-IL@ITO), respectively. It should be noted that the geometric area of bare ITO was equivalent to that of PS@ITO (or PS-IL@ITO). The coverage degree of electrospun PS and PS-IL films on the collecting screen was more than 99.5% based on calculation. The coverage degree of electrospun films was very high, and

the value can be further increased by prolonging the collecting time of electrospinning and optimizing the experimental parameters. It should be noted that the ionic liquid (BMIPF$_6$) used in our research was hydrophobic and immiscible with water, and there are strong interactions between the PS and the ionic liquid in the nanofibers. So the electrospun PS-IL film was very stable in the aqueous solution, which can been confirmed by the extremely stable cyclic voltammograms of PS-IL@ITO.

Superhydrophobicity and Conductivity Measurement. The wettability of a solid surface is a very important property that is governed by both the chemical composition and the geometrical microstructure of the surface.[3] Generally, the hydrophobicity of a solid surface can be improved by chemical modification, for example, through the incorporation of fluorine or silicone, as well as by increasing the roughness.[4,18,19] The high water repellence of superhydrophobic surfaces is attributed to the limited contact area between the solid and water which is manifested by a high static WCA and a low sliding angle.[4] Figure 4 shows the SEM images of electrospun PS film (a) and PS-BMIPF$_6$ composite film (c, 0.5% IL content) and the corresponding photographs taken during WCA measurements. The electrospun PS film consisting of regular nanofibers had a relatively flat surface, demonstrating a WCA of 141°, while the eletrospun PS-BMIPF$_6$ composite film consisting of branch-like microstructure showed a much rougher surface

(19) Feng, L.; Li, S.; Li, H.; Zhang, L.; Zhai, J.; Song, Y.; Liu, B.; Jiang, L.; Zhu, D. *Adv. Mater.* **2002**, *14*, 1857.
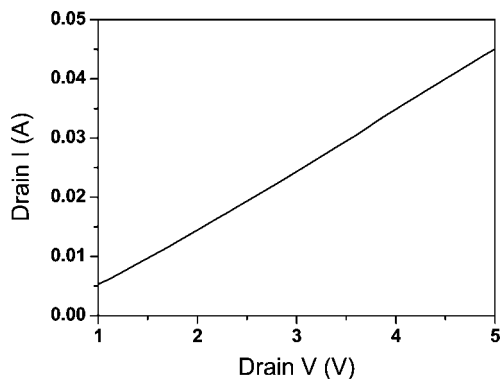
Figure 5. Typical *I−V* curve of electrospun PS-IL composite film on patterned ITO.

with an increased WCA of about 153°. The obtained PS-BMIPF$_6$ composite film was superhydrophobic. Moreover, a much smaller sliding angle (less than 10°) was obtained on the electrospun PS-BMIPF$_6$ composite film than on the PS film (more than 15°). Water droplets could roll easily on the electrospun PS-BMIPF$_6$ composite film surface with a slightly tilted angle. The elevated superhydrophobicity of electrospun PS-BMIPF$_6$ composite film can be elucidated by the following two aspects. First, the introduction of BMIPF$_6$ altered the electric charge in the original electrospinning solution, which further influenced the morphology of the elctrospun PS-BMIPF$_6$ composite film, resulting in increased roughness and hydrophobicity. The micro- and nanoscale hierarchical structures on the surface of the electrospun PS-BMIPF$_6$ composite film contributed to the superhydrophobicity. Second, BMIPF$_6$ has an intrinsic hydrophobic property; the entrapment of BMIPF$_6$ in PS fibers might also contribute to the superhydrophobicity of electrospun PS-BMIPF$_6$ composite film.

RTILs have intrinsic good conductivity. By entrapping BMIPF$_6$ in PS, the electrospun PS-IL composite film may also have good conductivity. The conductivity of the electrospun PS-BMIPF$_6$ sheet was measured by a sandwich structure using a Keithly 2400 source meter. Figure 5 shows the typical *I−V* curve of electrospun PS-IL composite film (0.5% IL content) on patterned ITO. The conductivity was calculated from the *I−V* measurement data for 10 samples. Thus, the conductivity can be calculated on the basis of the following equation:[8]

$$\sigma = \frac{d}{R_b S} \qquad (2)$$

where σ is the ionic conductivity, R_b the bulk resistance, d the thickness of electrospun PS-BMIPF$_6$ sheet, and S the geometric area of the measured sheet (0.25 cm^2), respectively. The bulk resistance R_b can be obtained from the *I−V* curve, and the thickness d can be estimated on the basis of cross-section measurement by SEM. The typical thickness of prepared PS-IL films was in the range of 75−85 μm with 25-min electrospinning periods. The average thickness of the samples for electrical measurements was 80 μm. The conductivity of the electrospun PS-BMIPF$_6$ sheet was calculated to be 3.2 × 10^{-4} S cm^{-1}. The good conductivity of superhydrophobic PS-BMIPF$_6$ composite film would be very effective for eliminating static-charge accumulation and may find potential applications in the fabrication of controllable and functional surface.

Conclusion

A PS-IL composite nanofiber was successfully prepared by an electrospinning method. The research revealed that the average diameter of the PS-IL nanofibers increased with the increased IL content in the original PS-IL solution. The dimension and morphology of electrospun films can be effectively controlled by altering the experimental parameters (especially the IL content) for electrospinning. The electrospun PS-IL composite film displayed both superhydrophobicity and conductivity, which may be ascribed to the micro- and nanoscale hierarchical structures of the electrospun PS-BMIPF$_6$ composite film and the intrinsic hydrophobicity and conductivity of BMIPF$_6$. Entrapment of IL within polymer by electrospinning provides a facile way to create IL-based nanofibers and composite film and may find wide potential applications in the fabrication of controllable and functional surface (such as antistatic self-cleaning coating and electronics).